

measurements.

<sup>1</sup>J. J. Rhyne, S. J. Pickart, and H. A. Alperin, *Phys. Rev. Lett.* **29**, 23, 1562 (1972).

<sup>2</sup>D. Pan and D. Turnbull, *J. Appl. Phys.* **45**, 3, 1406 (1974).

<sup>3</sup>A. Brenner, D. E. Couch, and E. K. Williams, *J. Res. Nat. Bur. Stand.* **44**, 109 (1950).

<sup>4</sup>P. Burlet, R. Chagnon, and P. Convert, Institut Laue-Langevin Instrument Description Report No. ID 2/73, 1973 (unpublished).

<sup>5</sup>R. M. Moon, *Int. J. Mag.* **1**, 219 (1971).

<sup>6</sup>T. E. Faber and J. M. Ziman, *Phil. Mag.* **11**, 153

(1965).

<sup>7</sup>To be published.

<sup>8</sup>W. Marshall and S. W. Lovesey, *Theory of Thermal Neutron Scattering* (Oxford Univ. Press, Oxford, England, 1971), p. 467.

<sup>9</sup>E. J. Lisher and J. B. Forsyth, *Acta Crystallogr., Sect. A* **27**, 545 (1971).

<sup>10</sup>A. W. Simpson and D. R. Brambley, *Phys. Status Solidi (b)* **43**, 291 (1971).

<sup>11</sup>J. F. Sadoc, J. Dixmier, and A. Guinier, *J. Non-Cryst. Solids* **12**, 46 (1973).

<sup>12</sup>C. S. Cargill, III, and R. W. Cochrane, in *Amorphous Magnetism*, edited by H. O. Hooper and A. M. de Graaf (Plenum, New York, 1973) p. 313.

### $|g_A/g_V|$ in the Decay $\Sigma^- \rightarrow ne^- \bar{\nu}$

W. Tanenbaum, V. Hungerbuehler,\* R. Majka, J. Marx, P. Nemethy, J. Sandweiss, and W. Willis†  
*Yale University, New Haven, Connecticut 06520‡*

and

M. Atac, S. Ecklund, P. J. Gollon, J. Lach, J. MacLachlan, A. Roberts, R. Stefanski, and D. Theriot  
*National Accelerator Laboratory, Batavia, Illinois 60510§*

and

C. L. Wang  
*Brookhaven National Laboratory, Upton, New York 11973 ||*  
(Received 11 March 1974)

The decay  $\Sigma^- \rightarrow ne^- \bar{\nu}$  was studied using a hyperon beam at the Brookhaven alternating-gradient synchrotron. The  $\Sigma^-$  and  $e^-$  momenta were measured by magnetic spectrometers with magnetostrictive wire spark chambers. A threshold Cherenkov counter and a total-absorption calorimeter identified the electron and neutron, respectively. From a sample of 3507 reconstructed events we have found  $|g_A/g_V| = 0.435 \pm 0.035$ .

We report a measurement of the magnitude of the ratio of the axial vector to vector form factors,  $|g_A/g_V|$ , from the observation of 3507 decays of the type  $\Sigma^- \rightarrow ne^- \bar{\nu}$ . These events were produced using the Yale University-National Accelerator Laboratory-Brookhaven National Laboratory high-energy negative hyperon beam at the Brookhaven National Laboratory alternating-gradient synchrotron.<sup>1</sup> The hyperon beam delivers a flux of approximately 200  $\Sigma^-$  per machine pulse, produced in the forward direction, at a central momentum of 23 GeV/c at the exit of the magnetic channel. Figure 1 depicts the beam and the associated electronic detection apparatus which are described in more detail elsewhere.<sup>1</sup> Beam particles of mass less than that of a proton are vetoed by a threshold Cherenkov counter ( $C_B$ ) which forms part of the beam channel, and are also vetoed by a scintillation counter located at the down-

stream end of the apparatus. A cluster of high-pressure, high-resolution magnetostrictive spark chambers<sup>2</sup> determine the momentum of the emerging hyperons to 1%. A set of small counters on either side of these chambers ( $B$ ) and a hole veto counter ( $V_H$ ) define the beam and discriminate against upstream hyperon decays.

Located downstream of the 115-in. decay region is a magnetic spectrometer with conventional magnetostrictive wire spark chambers which determines the momentum of the electron from the decay  $\Sigma^- \rightarrow ne^- \bar{\nu}$  to about 5%. Situated after the spectrometer is a Cherenkov counter ( $C$ ) filled with hydrogen at atmospheric pressure. This counter, which has a large phase-space acceptance, identifies electrons from the desired leptonic decay among the more copious pions produced in the major decay mode,  $\Sigma^- \rightarrow n\pi^-$ . This counter suppresses the trigger rate for the major

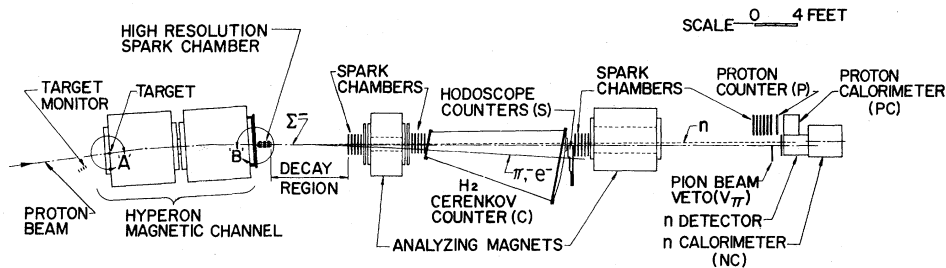


FIG. 1. Schematic diagram of the high-energy hyperon beam.

decay mode by a factor of approximately 80. Following the Cherenkov counter is a hodoscope of scintillation counters (S), each of which shadows one of the five optical cells of the electron Cherenkov counter. In addition, the counter nearest to the beam line is backed by a lead and scintillator shower counter to give extra discrimination against nonleptonic backgrounds.

A multiplate, proportional-chamber, scintillator neutron detector<sup>3</sup> is situated downstream of the second spectrometer magnet and provides a measure of the decay-neutron direction to 1 mrad. The hadron calorimeter (NC) is used to discriminate against background muons by requiring a minimum pulse height in the trigger. The crude information on the neutron energy ( $\pm 25\%$ ) is not used in the reconstruction.

The decay  $\Sigma^- \rightarrow ne^- \bar{\nu}$  was signified by the trigger

$$\bar{C}_B B \bar{V}_H C S (NC) \bar{V}_\pi.$$

Two-body decays,  $\Sigma^- \rightarrow n\pi^-$ , and beam pions were also recorded at a scaled-down rate to provide a flux normalization and to monitor the efficiency and resolution of the chambers and neutron detector. The total trigger rate was a few per machine pulse. For each trigger we recorded the configuration of scintillation-counter hits, the pulse heights from the electron Cherenkov counter, shower counter, and hadron calorimeter, and the time difference between signals from the electron Cherenkov counter and the S counter hodoscope, as well as the spark-chamber and multiwire-proportional-chamber information. The major source of background in the leptonic trigger came from the decay  $\Sigma^- \rightarrow n\pi^-$  in coincidence with a background muon which triggered the electron Cherenkov counter. A major task of the analysis was to remove this background (which is thrice over-constrained) from the signal of leptonic decays.

Figure 2(a) shows the beam mass spectrum of events with a decay angle of greater than 9 mrad

when reconstructed under the hypothesis  $\Sigma^- \rightarrow n\pi^-$ . The broad distribution contains the leptonic events and the sharp peak at the  $\Sigma^-$  mass contains the two-body background. A reduction of the nonlep-

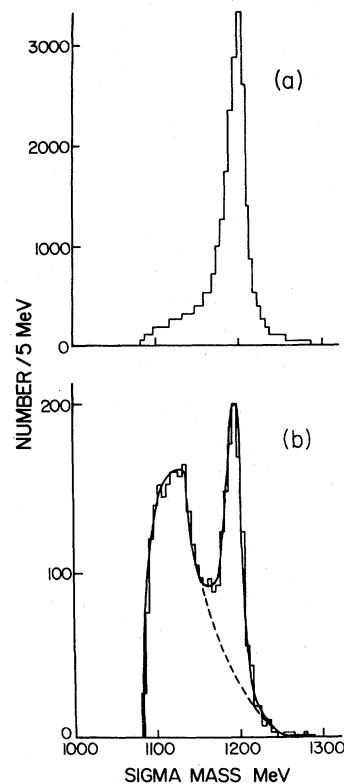


FIG. 2. (a) Mass spectrum of beam particles for leptonic decays at an early stage of the analysis when reconstructed under the hypothesis  $\Sigma^- \rightarrow n\pi^-$ . The leptonic events being sought are in the broad tail; the two-body background events are in the sharp peak. (b) The same spectrum at the last stage in the analysis. The smooth curves indicate the shapes predicted by the Monte Carlo calculation: dashed,  $\Sigma^- \rightarrow nev$  only; solid,  $\Sigma^- \rightarrow nev$  plus  $\Sigma^- \rightarrow n\pi^-$ . A final mass cut of 1165 MeV was made and events below that mass were considered to be leptonic decays.

TABLE I. Results for  $|g_A/g_V|$  and the maximum value of likelihood fits from neutron spectrum in the c.m. system.

Spectrometer field integral	$ g_A/g_V $	$\ln \mathcal{L}(\text{data})$	$\ln \mathcal{L}(\text{Monte Carlo})$	Probability $\mathcal{L}(\text{Monte Carlo}) < \mathcal{L}(\text{data})$
6 kG m	$0.420 \pm 0.045$	-51.68	$-53.28 \pm 3.26$	69%
13 kG m	$0.455 \pm 0.055$	-52.11	$-49.62 \pm 3.18$	22%

tonic background was made by requiring a large pulse height in the shower counter when relevant, a proper time difference between the electron Cherenkov counter and appropriate  $S$  counter, and that the reconstructed negative track point to the proper cell of the Cherenkov counter and the proper  $S$  counter. These consistency requirements serve to define decay electrons and eliminate events having a background muon triggering the electron Cherenkov counter, reducing the non-leptonic backgrounds to the level depicted in Fig. 2(b). The smooth curve in Fig. 2(b) indicates the excellent agreement between the data and the spectrum as generated by a Monte Carlo calculation. The final sample of 3507  $\Sigma^- \rightarrow ne^- \bar{\nu}$  decays results from a cut requiring the reconstructed  $\Sigma^-$  mass, assuming the hypothesis  $\Sigma^- \rightarrow n\pi^-$ , to be less than 1165 MeV.

Since for this leptonic decay there is a square-root ambiguity resulting from the zero-constraint fit, we cannot assign an event a unique position on a Dalitz plot. In order to obtain the maximum information in a bias-free manner, both solutions were kept and each event plotted on a three-dimensional Dalitz plot. The electron energy and two neutron energies define the coordinates. The form-factor ratios were obtained from the final event sample by a maximum-likelihood fit to projections of the three-dimensional "Dalitz plot" weighted by a Monte Carlo calculation of the acceptance of the detection apparatus. Our c.m. neutron and electron energy resolution (about 5 MeV) corresponds to five neutron energy bins for each solution and twenty electron energy bins.

Data were taken for two values of the magnetic field in the spectrometer magnet. The two results for the absolute value of the form-factor ratio as computed from a likelihood-function ( $\mathcal{L}$ ) fit to the neutron spectrum only are presented in Table I. In obtaining these results, it was assumed that second-class currents are negligible and that the effect of weak magnetism is that predicted by the conserved-vector-current hypothe-

sis. The result is quite insensitive to the amount of weak magnetism present. The full two-dimensional neutron spectrum was used in the actual maximum-likelihood fit. We can also construct a one-dimensional spectrum by giving both solutions equal weight. Figure 3 shows the resulting neutron spectrum for the 6-kG-m data compared with expected spectra for  $|g_A/g_V| = 0.3$  and  $|g_A/g_V| = 0.5$ . We present this comparison to give a visual indication of the sensitivity of the measurement.

The quality of the likelihood fit described above was evaluated with standard Monte Carlo techniques, and the results of this evaluation are presented in Table I. The detection efficiency calculated for leptonic decays was 11%. Most of the loss was due to  $\Sigma^-$  decaying upstream of the fiducial region or to decay electrons hitting the

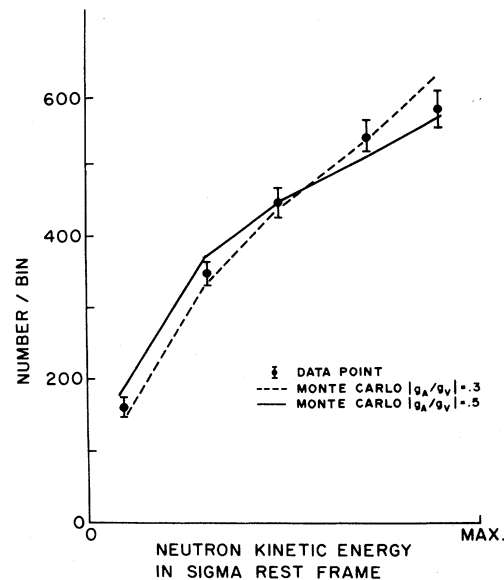


FIG. 3. A comparison of the experimentally determined neutron c.m. energy spectrum and those expected for two values of  $|g_A/g_V|$ . Both solutions for the energy are used with equal weight.

TABLE II. Summary of  $\Sigma^- \rightarrow ne^- \bar{\nu}$  form-factor experiments.

Experiment	Year	No. of Events	$ g_A/g_V $
Maryland <sup>a</sup>	1969	49	0.23 ± 0.16
Heidelberg <sup>b</sup>	1969	33	0.37 $^{+0.26}_{-0.19}$
Columbia-Stony Brook <sup>c</sup>	1972	36	0.29 $^{+0.28}_{-0.23}$
This experiment	1973	3507	0.435 ± 0.035

<sup>a</sup>Ref. 5<sup>b</sup>Ref. 6.<sup>c</sup>Ref. 7.

spectrometer magnet. The probability of a decay electron hitting the spectrometer magnet was extremely weakly correlated with the neutron c.m. energy. The size of the neutron detector was chosen to intercept 100% of the neutrons. The efficiency of neutron detection was independent of angle and only weakly dependent on laboratory momentum (less than 5% variation). The detection efficiency was thus almost entirely independent of the neutron c.m. energy.

The errors assigned to  $|g_A/g_V|$  are purely statistical. However, none of the small systematic corrections considered contributes significant uncertainties. The  $\Sigma^- \rightarrow n\pi^-$  background contamination after the mass cut was 1.5% of the leptonic sample for the 6-kG-m data. This was determined by looking at the mass spectrum of real  $\Sigma^- \rightarrow n\pi^-$  events. This background was included in the Monte Carlo simulation. The result for  $|g_A/g_V|$  was found to be insensitive to such background of up to 10%. The final result for the absolute value of the form-factor ratio is obtained by averaging the results from the two data samples to yield

$$|g_A/g_V| = 0.435 \pm 0.035.$$

It is interesting to note that the Cabibbo theory<sup>4</sup> predicts  $g_A/g_V = 0.33 \pm 0.04$ . Table II contains a comparison of this experiment with the results of previous experiments.

We wish to thank our engineering staff, Andy Disco, Satish Dhawan, Cordon Kerns, Stan Ladinski, Blaise Lombardi, and Irving Winters, and our technicians Alan Wandersee, Jon Blomquist, and Ed Steigmeyer for their help in the design and setup of the apparatus. We also thank the alternating-gradient synchrotron staff, in particular David Berley, Eugene Halek, and Gerry Tanguay, for providing the technical support needed for the success of this experiment.

\*Present address: Université de Genève, Genève, Switzerland.

†Present address: CERN, Geneva, Switzerland.

‡Research supported by the U. S. Atomic Energy Commission under Contract No. AT(11-1).

§Operated by Universities Research Association Inc. under contract with the U. S. Atomic Energy Commission.

||Research supported in part by the U. S. Atomic Energy Commission.

<sup>1</sup>V. Hungerbuehler *et al.*, Nucl. Instrum. Methods **115**, 221 (1974).

<sup>2</sup>W. J. Willis *et al.*, Nucl. Instrum. Methods **91**, 33 (1971).

<sup>3</sup>M. Atac *et al.*, Nucl. Instrum. Methods **106**, 263 (1973).

<sup>4</sup>H. Ebenhoeh *et al.*, Z. Phys. **241**, 473 (1971).

<sup>5</sup>A. P. Colleraine *et al.*, Phys. Rev. Lett. **23**, 198 (1969).

<sup>6</sup>F. Eisele *et al.*, Z. Phys. **223**, 487 (1969).

<sup>7</sup>C. Baltay *et al.*, Phys. Rev. D **5**, 1569 (1972).